Research Square

Preprints are preliminary reports that have not undergone peer review.
They should not be considered conclusive, used to inform clinical practice,
or referenced by the media as validated information.

Breaking the nexus between yield and carotenoid levels in sweet potato: Development of improved cultivars and identification of key improvement genes

Haipeng Li
Henan University
Yangcang Gong
Hunan Academy of Agricultural Sciences
Penglong Zhang
Henan University
Jingru Li
Henan University
Yanguo Feng
Henan University
Kun Li
Henan University
Zongyan Chu
Henan University
Meimeng Yang
Henan University
Kun-Peng Jia
Henan University
José Ramón Botella
University of Queensland
Wei Wang
Institute of Henan Yifengnian Sweet Potato Science
Yongyue Zhang
Luohe Academy of Agricultural Sciences
Yuli Du
Henan University
Jinggong Guo
jgguo@henu.edu.cn

Henan University

Research Article

Keywords: Sweet potato, Storage root, Carotenoids, Variety development, IbGGPPS2

Posted Date: April 4th, 2026

DOI: https://doi.org/10.21203/rs.3.rs-9030226/v1

License: This work is licensed under a Creative Commons Attribution 4.0 International License.
Read Full License

Additional Declarations: No competing interests reported.

Version of Record: A version of this preprint was published at BMC Plant Biology on June 18th, 2026. See the published version at https://doi.org/10.1186/s12870-026-09159-5.

Abstract

Sweet potato (*Ipomoea batatas* (L.) Lam) is a globally important staple crop with high nutritional value, yet most commercial cultivars exhibit a trade-off between yield and carotenoid content. To address this limitation, we used a hybrid population of 27 elite varieties to undergo open pollination and identified two novel lines, XZ 8 − 1 and LS 9 − 1 with improved agronomic traits. XZ 8 − 1 showed a 40-fold increase in carotenoid content compared to its maternal line, while LS 9 − 1 maintained the high carotenoid levels of the maternal line but showed significantly improved yield. Molecular analysis revealed that *IbGGPPS2*, a geranylgeranyl diphosphate synthase gene, was highly expressed in the high-carotenoid line XZ 8 − 1. Bacterial complementation assays confirmed that *IbGGPPS2* encodes a protein with geranylgeranyl diphosphate synthase activity. Functional validation via heterologous expression in *Arabidopsis* and overexpression in sweet potato confirmed that IbGGPPS2 enhances carotenoid biosynthesis and has a strong positive effect on plant growth. Our findings provide a promising strategy for the simultaneous improvement of nutritional quality and yield in sweet potato breeding programs.

Introduction

Sweet potato (*Ipomoea batatas* (L.) Lam.), a member of the Convolvulaceae family, ranks as the seventh most important food crop globally [1, 2]. In China, sweet potato is the fourth largest staple crop by production, significantly contributing to food security and agricultural sustainability [3, 4]. The tuberous roots are not only rich in starch and dietary fiber but also serve as a valuable source of health-promoting compounds such as β-carotene and anthocyanins [5, 6]. Genetic research into sweet potato is challenging due to its hexaploid genome (2n = 6x = 90), low seed set, and complex polyploid interactions [7–10]. Available cultivars exhibit a range of flesh colors—white, yellow, orange, and purple—and even though all varieties contain β-carotene and other carotenoids; orange-fleshed types are particularly rich in β-carotene [11].

Carotenoids are essential terpenoid pigments with critical roles in a broad spectrum of organisms, including plants, animals, and microorganisms [12]. In plants, they function as accessory pigments in photosynthesis, protect against photo-oxidative damage, and enhance stress tolerance [13–16]. They also contribute to flower and fruit color, aiding in pollination and seed dispersal [17]. In humans, carotenoids provide antioxidant benefits, help prevent chronic diseases, and support immune function [18–20]. β-Carotene, in particular, serves as a vitamin A precursor, making β-carotene-rich crops like orange-fleshed sweet potato a dietary solution to combat vitamin A deficiency [21–23]. Additionally, β-carotene is a metabolic precursor for other nutritionally important carotenoids [24, 25].

The biosynthesis of carotenoids begins with the condensation of isopentenyl diphosphate (IPP) and dimethylallyl diphosphate (DMAPP), derived from the mevalonate (MVA) and methylerythritol phosphate (MEP) pathways [26, 27]. Geranylgeranyl diphosphate synthase (GGPPS) catalyzes the formation of geranylgeranyl diphosphate (GGPP), a key isoprenoid precursor [28, 29]. Phytoene synthase then converts GGPP to phytoene, which is subsequently desaturated and isomerized to lycopene [30, 31].

Lycopene represents a key metabolic branch point, being cyclized by lycopene ε-cyclase (LCYE) and β-cyclase (LCYB) to form α-carotene, or by LCYB alone to produce β-carotene. These primary carotenes are further modified into xanthophylls such as lutein, zeaxanthin, and violaxanthin [32, 33].

Although sweet potato carotenoids hold substantial nutritional and economic value, most commercial cultivars face a trade-off between high yield and high carotenoid content. To address this limitation, we developed a hybrid population of 27 elite varieties under short-day conditions in Sanya, China. Our analysis revealed a clear gradient in carotenoid content: orange-fleshed > yellow-fleshed > white-fleshed > purple-fleshed. Through open pollination, we obtained two new varieties with significantly improved carotenoid content, storage root size, and yield compared to their maternal parents. Subsequent molecular analysis and functional characterization identified a carotenoid biosynthesis gene, IbGGPPS2 with a key role in enhancing plant growth and carotenoid accumulation. Our integrated breeding approach demonstrates the potential to simultaneously improve nutritional quality and agronomic performance in sweet potato.

Materials and methods

Plant materials

All sweetpotato cultivars mentioned in this study are widely planted commercial varieties, cited under their common names (Shangshu 23, Fucaishu 18, Jishu 33, Longshu 9, Yanshu 25, Sushu 33, Pushu 32, Yusi 1, Zhenghong 35, Hongyao, Qixu 37, Xiangshu 628, Chuanshu 294, Zheshu 13, Luoshu 17, Qining 427, Longzi 221, Xuzishu 8, Sushu 28, Sushu 45, Hami, Luoshu 16, Shangshu 19, Xushu 37, Aozhouzibai, Xuzishu 13, Zijingxiang), as specified in the text.

Arabidopsis thaliana plants were grown in a walk-in growth chamber at a temperature of 22 ± 1°C, with a 16/8 h light/dark photoperiod and a light intensity of 120 μmol m^{-2} s^{-1}.

The sweet potato hybridization was conducted at the South Breeding Base of Henan University (Sanya, Hainan Province, China). Prior to cultivation, ridges were formed and covered with plastic film with a spacing of 40 cm between them. A complex amino acid compound fertilizer was applied as a base fertilizer in a single dose. The plants were arranged in fixed rows with a spacing of 25 cm between plants.

Seeds from open pollination were sown in seedling trays containing a sterilized 1:1 mixture of potting soil and vermiculite at a density of 2 × 3 cm. Plants were maintained under 28–30/22–25°C day/night temperatures with 70% − 75% humidity. When seedlings reached 12 ± 2 cm height with 4–5 true leaves, they were transplanted to the field with soil at a 50×30 cm spacing and shaded for 3 d. Agronomic traits were recorded during critical growth stages, and superior individuals were selected based on carotenoid content. Finally, selected genotypes were clonally propagated through cuttings to stabilize the desired characteristics.

The Sweet potato *IbGGPPS2*-overexpressed transgenic plants were cultivated outdoors (Sanya, Hainan Province, China) with natural light and a temperature of 25–31°C. Each transgenic plant was cultivated in a 5-gallon pot and each transgenic line contained at least ten plants.

HPLC-PDA analysis of carotenoids

Sample Preparation: Fresh sweet potato slices were frozen in liquid nitrogen and lyophilized. Powdered sample (100 mg) was saponified with 2 mL of 95% ethanol, 1 mL of 300 mM NaCl, 4 mL of 500 mM pyrogallol, 1 mL of 1 M ascorbic acid, and 2 mL of 10.7 M KOH under nitrogen at 70°C for 45 min. After cooling on ice, the reaction was quenched with 0.75 mL of 3 M NaCl. The mixture was extracted thrice with 15 mL of hexane/ethyl acetate (9:1, v/v). The combined organic layers were washed, dried over Na_2SO_4, concentrated under N_2, and reconstituted in 2 mL hexane. The solution was filtered through a 0.22 μm organic membrane into an amber vial.

HPLC Analysis: Analysis was performed on a C30 column (YMC, 4.6 × 150 mm) at 25°C. Mobile phase A was methanol-water (97:3) with 0.05 M ammonium acetate and 0.1% BHT, and phase B was MTBE with 0.1% BHT. The gradient was: 0 min (90% A); 0–18 min (80% A); 18–20 min (50% A); 20–25 min (10% A); 25–29 min (10% A); 29-29.5 min (90% A); 29.5–40 min (100% A). Flow rate was 1.0 mL/min. Detection used a PDA detector at 450 nm, with all steps protected from light.

Analysis of nutritional quality parameters in sweet potato tubers

Determination of Total Carotenoid Content in Sweet Potato Tubers. Fresh tuber homogenate (1.0 g) was extracted repeatedly with ice-cold acetone-petroleum ether (1:1, v/v) under dark conditions until the residue became colorless. The combined extracts were diluted to 50 mL, and absorbance was measured at 450 nm. Carotenoid content was calculated as (A × V) / (E × W), where A is the absorbance, V is the total volume (mL), E is 2592, and W is the sample fresh weight (g).

Determination of Dry Matter Content. Uniformly sliced fresh samples were dried at 55°C to constant weight. Dry matter content was calculated as the ratio of dry weight to fresh weight multiplied by 100.

Analysis of Reducing and Total Sugars. For reducing sugars, 1 g fresh sample was homogenized, boiled to inactivate enzymes, and centrifuged. For total sugars, 0.5 g sample was acid-hydrolyzed with 6 M HCl and neutralized. Both extracts were reacted with DNS reagent, and absorbance at 540 nm was measured. Sugar content was calculated as (C × V × D × 100) / (W × 10^6), where C is glucose concentration (μg/mL), V is volume (mL), D is dilution factor, and W is sample weight (g).

Determination of Starch Content. After removing soluble sugars with 80% ethanol, samples were gelatinized and acid-hydrolyzed. The hydrolysate was reacted with anthrone-sulfuric acid reagent, and absorbance at 620 nm was measured. Starch content was calculated as (C × V × 0.9 × 100) / (m × 10^6), where C is glucose concentration (μg/mL), V is volume (mL), and m is sample mass (g).

Analysis of Soluble Protein Content. Samples were homogenized in PBS buffer and centrifuged. The supernatant was reacted with Coomassie Brilliant Blue G-250, and absorbance at 595 nm was measured. Protein content was determined as (C × V × D) / (m × 1000), where C is protein concentration (μg/mL), V is volume (mL), D is dilution factor, and m is sample mass (g).

Phylogenetic analysis

The amino acid sequences of 6 IbGGPPS-LSU and 2 IbGGPPS-SSU isoforms were retrieved from the Taizhong 6 genome database (http://sweetpotao.com). Additionally, full-length GGPPS amino acid sequences previously reported in Arabidopsis thaliana, Nicotiana tabacum, Oryza sativa, *Gossypium spp.*, Solanum lycopersicum, and Capsicum annuum were obtained from their respective genome databases. Multiple sequence alignment was performed using MEGA 11, and a phylogenetic tree was constructed by the Neighbor-Joining method. The resulting evolutionary tree was visualized and annotated using the Interactive Tree of Life (iTOL) platform.

RT-qPCR analysis

RNA isolation was performed using the RNAprep Pure Plant kit (Tiangen) on 90-d storage roots of XZ 8 − 1 and YS 25 for gene discovery, on PS 32 storage roots at 60, 75, 90, 105, and 120 d for *IbGGPPS2* expression profiling, on 90 d storage roots, young stems, leaves, and flowers of PS 32 for *IbGGPPSs* expression comparison, and on 60 d storage roots of overexpressing plants for transgene validation. Total RNA (1 μg) was reverse-transcribed into cDNA using the HiScript II Q Select RT SuperMix (Vazyme). Quantitative real-time PCR (qPCR) was then performed with the ChamQ SYBR Color qPCR Master Mix (Vazyme) on a Roche LightCycler 480 instrument. The thermal cycling protocol consisted of an initial denaturation at 95°C for 2 min, followed by 40 cycles of denaturation at 95°C for 15 sec and annealing/extension at 60°C for 30 sec.

Bacterial color complementation assay

The recombinant pET32b-IbGGPPS vector was co-transformed with the pAC-94N vector into Escherichia coli BL21 competent cells to enable β-carotene biosynthesis. When functionally active GGPPS is co-expressed with pAC-94N, the carotenoid biosynthesis pathway is reconstituted, leading to β-carotene accumulation and conferring a characteristic yellow phenotype to the colonies. The experimental procedure was as follows: Positive clones were selected and cultured in LB medium supplemented with ampicillin (50 μg/mL) and chloramphenicol (50 μg/mL). When the culture reached an OD600 of 0.6, recombinant protein expression was induced with 1 mM isopropyl-β-D-thiogalactoside (IPTG) at 16–20°C for 20 h. After centrifugation, color differences in the pellet were observed. Subsequently, 720 μL of acetone was added to extract the pigments. Once the pellet turned white, 180 μL of ultrapure water was added, followed by centrifugation to collect the supernatant. The absorbance of the supernatant was measured at 440 nm using a microplate reader.

Heterologous overexpression of Arabidopsis thaliana

The *IbGGPPS2* gene was cloned into the hygromycin-resistant pCAMBIA1300-GFP vector to generate the *35S::IbGGPPS2:GFP* recombinant overexpression construct. This construct was subsequently introduced into *Agrobacterium tumefaciens* GV3101. Bacterial cells from antibiotic-selected cultures were collected and resuspended in a 1/2 MS solution containing 5% sucrose and 0.03% Silwet-77, adjusted to an OD600 of 1.0, which served as the inoculation medium. Floral buds of 4–6-week-old *Arabidopsis* plants were immersed in this bacterial suspension for 45 seconds, followed by 16 h of dark incubation and subsequent recovery under normal growth conditions. T1 seeds were harvested and screened on hygromycin-supplemented MS medium. Positive transformants were confirmed by PCR with gene-specific and GFP-tag primers and further validated by sequencing. Homozygous lines were then generated and advanced for phenotypic characterization.

In planta transformation of sweet potato stem segments

The in planta transformation of sweet potato stem segments was conducted using Agrobacterium tumefaciens strains EHA105/AGL1 and K599. Bacterial cultures were grown in LB medium supplemented with kanamycin and either rifampicin or streptomycin at 28°C with shaking until OD600 reached 0.8-1.0. Fresh apical stem segments (25–30 cm) were selected, with basal leaves and adventitious roots removed, and nodes were punctured to facilitate infection. The prepared stems were immersed in bacterial suspension for 8–12 h under gentle agitation. After infection, stems were co-cultivated in distilled water in the dark for 24 h. Subsequently, a 200 mg/L carbenicillin solution was applied for 1 h with gentle shaking to eliminate residual bacteria, followed by two distilled water rinses. Finally, the treated stems were transplanted into well-watered field soil with transplantation dates recorded [34].

Chlorophyll extraction and quantification

Fresh tissue (0.1 g) was homogenized in an ice bath, then centrifuged at 4,000 rpm for 10 min at 4°C. The supernatant was collected and filtered through a 0.45 μm membrane. Absorbance was measured at 663 nm and 645 nm using 80% acetone as blank. All measurements were performed in triplicate. Chlorophyll concentrations were calculated as follows: Total chlorophyll = $7.15\times A_{663} + 18.71\times A_{645}$.

Photosynthesis Measurements

Under high light (1250 μmol photons m^{-2} s^{-1}) for 2 h, *IbGGPPS2* overexpressing sweet potato plants were analyzed alongside controls under normal light (350 μmol photons m^{-2} s^{-1}). Using an IMAGING-PAM-MAXI system at 25°C, the maximum quantum yield of PSII (F_v/F□) and non-photochemical quenching were measured following established protocols [35]. The electron transfer rate (ETR) was determined after 2 min of actinic light exposure at increasing intensities (20 to 1100 μmol photons m^{-2} s^{-1}) by

recording steady-state fluorescence (F□) and light-adapted maximum fluorescence (F□'). ETR was calculated as Y(II) × PAR × 0.5 × 0.84, where Y(II) = (F□' − F□)/F□' [36].

Results

Characterization of a natural hybrid sweet potato population

To facilitate the breeding of high-carotenoid sweet potato varieties, we established a genetically diverse hybrid population comprising 27 accessions with 4 distinct flesh-color groups: orange-red (9), yellow (7), white (7), and purple (4) (Supplemental Fig. S1). All accessions exhibited pollen viability ranging from 10% to 44%, confirming their potential as effective parents in hybridization schemes (Supplemental Fig. S2). To assess carotenoid profiles across color groups, we quantified β-carotene, xanthophyll, and zeaxanthin in representative accessions from each group (Fig. 1). As expected, orange-red fleshed tubers contained the highest β-carotene levels (Fig. 1A), followed by yellow-fleshed types (Fig. 1C), whereas white and purple fleshed materials showed markedly lower β-carotene content (Fig. 1E, G), thereby establishing a positive correlation between β-carotene content and the deepening of flesh color across the spectrum from white to yellow to orange. Moreover, only orange-red fleshed accessions contained both xanthophyll and zeaxanthin (Fig. 1B). Among yellow fleshed materials, by contrast, only a subset accumulated either xanthophyll or zeaxanthin (Fig. 1D), while white-fleshed genotypes completely lacked both (Fig. 1F). Intriguingly, purple-fleshed tubers did not accumulate xanthophyll but contained zeaxanthin at levels comparable to those observed in orange-red accessions (Fig. 1H). Phenotypic observations of leaf morphology revealed additional diversity, with accessions exhibiting either heart-shaped or pinnate leaves with varying green pigmentation intensity (Supplemental Fig. S3), suggesting possible differences in photosynthetic performance.

In summary, the assembled hybrid population shows marked genetic diversity across multiple traits, including tuber pigmentation, pollen fertility, carotenoid composition and leaf morphology. Collectively, these features qualify the population as a valuable resource for sweet potato breeding via open pollination strategies.

Development of the high-carotenoid, high-yield sweet potato varieties XZ 8 − 1 and LS 9 − 1

Two novel sweet potato varieties, XZ 8 − 1 (derived from maternal parent Xuzishu 8; XZ 8) and LS 9 − 1 (derived from maternal parent Longshu 9; LS 9), were produced via open-natural hybridization, with each exhibiting distinct and complementary agronomic improvements over the high-carotenoid, high-yielding control cultivar YS 25. Visually, XZ 8 − 1 displayed a striking shift in tuber flesh coloration, transitioning from the purple of the maternal parent XZ 8 to a deep orange-red hue that surpassed even the intense coloration of YS 25 (Fig. 2A-C). In contrast, LS 9 − 1 maintained an orange flesh color similar to both its parent and YS 25.

Quantitative phytochemical profiling showed that total carotenoid content in XZ 8 − 1 was dramatically higher than its parent (40-fold) and 50% higher than YS 25 levels (Fig. 2D). Although LS 9 − 1 showed a slight reduction in carotenoids relative to its parent, LS 9 − 1 levels were indistinguishable from the high benchmark set by YS 25 (Fig. 2D). Further compositional analysis revealed different sugar profiles: XZ 8 − 1 showed no significant differences in reducing sugar content compared to its parent but had a significant increase in total sugar (Fig. 2E-F). LS 9 − 1, however, exhibited a marked rise in reducing sugars compared with its LS 9 parent, matching the levels in YS 25, while total sugar content did not differ significantly among LS 9 − 1, its parent, and the control (Fig. 2E-F). Regarding other key quality traits, XZ 8 − 1 proved stable, showing no significant differences from its parent in dry matter, starch, or protein content (Fig. 2G-I). LS 9 − 1, meanwhile, displayed a more complex profile, with dry matter content similar to its parent, decreased starch content and increased protein content (Fig. 2G-I).

Critically, both varieties demonstrated enhanced yield attributes, albeit through different means. For XZ 8 − 1, although tuber number per plant was reduced relative to its parent and similar to YS 25, the total tuber fresh weight per plant remained unchanged, suggesting a compensatory increase in individual tuber size (Fig. 2J-K). LS 9 − 1, by contrast, achieved a clear quantitative yield leap, with significant increases in tuber number (~ 24%) and fresh weight (~ 20%) per plant compared to its parent (Fig. 2J-Q). The yield improvements were underpinned by favorable morphological changes: XZ 8 − 1 showed increased vine length, stem diameter, and leaf area, whereas LS 9 − 1 exhibited enhanced leaf area and branch number (Supplemental Fig. S4).

In summary, the two new varieties provide distinct breeding achievements. XZ 8 − 1 constitutes a qualitative breakthrough, characterized by its dramatically enhanced carotenoid content and deep pigmentation, making it an elite cultivar suited for premium nutraceutical markets. LS 9 − 1, on the other hand, provides a quantitative leap, combining high carotenoid levels with significantly improved yield, thus offering strong potential for large-scale, high-efficiency cultivation.

Identification of IbGGPPS2 as a putative key regulator of carotenoid accumulation in sweet potato tubers

To elucidate the molecular determinants of carotenoid accumulation in sweet potato storage roots, we performed transcriptional profiling of key carotenoid metabolic genes across multiple cultivars and their derivatives: XZ 8 (purple-red tubers), its derived line XZ 8 − 1 (orange-red tubers, extremely high carotenoid content), LS 9 (orange tubers), its derived line LS 9 − 1 (orange tubers), and YS 25 (orange tubers) (Fig. 2). The qRT-PCR results indicated that *IbGGPPS2* exhibited the most dramatic expression differences among all examined genotypes and genes, including other *IbGGPPSs* and key node genes in the carotenoid metabolic pathway. Notably, *IbGGPPS2* expression in XZ 8 − 1 was not only 15-fold higher than in YS 25, but also showed a striking 195-fold increase compared to its parent XZ 8. Furthermore, *IbGGPPS2* expression in LS 9 − 1 was elevated 7.5-fold relative to its parent LS 9, reaching a level comparable to that in YS 25, and again exhibited the greatest increase among all genes analyzed. The

expression analysis suggest that *IbGGPPS2* is a critical contributor to the enhanced carotenoid biosynthesis observed in XZ 8 − 1 tubers.

To gain evolutionary and functional context, we performed a phylogenetic analysis of GGPPS proteins across diverse plant species. The 6 identified *IbGGPPS* members segregated into two distinct subfamilies (Fig. 3B). Significantly, *IbGGPPS1, IbGGPPS2, IbGGPPS3*, and *IbGGPPS6* clustered within subfamily III, a group that includes well-characterized, fruit-specific carotenoid biosynthetic genes such as tomato *SlGGPPS2* (responsible for lycopene and β-carotene accumulation) and pepper *CaGGPPS1* (involved in capsanthin biosynthesis) [29, 30]. This phylogenetic association suggests a shared and specialized role for these IbGGPPS members in facilitating carotenoid production in storage organs. In contrast, *IbGGPPS4* and *IbGGPPS5* formed a separate clade, subfamily IV, grouping with tomato *SlGGPPS1* (Fig. 3B), a gene known for its primary role in chlorophyll metabolism and maintaining photosynthetic efficiency [37], thereby implying a divergent, photosynthesis-related function for these paralogs.

We next sought to experimentally validate the enzymatic activity of the candidate genes. Using a bacterial pigment complementation assay, where functional GGPPS catalysis leads to β-carotene production and yellow pigmentation [29, 38], we assessed the capacity of several IbGGPPS enzymes to catalyze the production of β-carotene. Consistent with its being the most highly expressed member among the examined *IbGGPPS* genes, *IbGGPPS2* conferred the most intense yellow coloration to the bacterial colonies, with *IbGGPPS4* and *IbGGPPS6* also producing yellow color although at lower intensity; while *IbGGPPS1* and *IbGGPPS5* failed to produce yellow colonies (Fig. 3C). The visual assessment was quantitatively confirmed by spectrophotometry, suggesting that IbGGPPS2 has GGPPS enzymatic activity (Fig. 3D).

To further explore the role of IbGGPPS2 in carotenoid accumulation *in planta*, we studied its expression profile. Tissue-specific analysis revealed that *IbGGPPS2* transcripts were considerably more abundant than those of *IbGGPPS4* and *IbGGPPS6* across all major tissues, including tubers, stems, leaves, and flowers (Fig. 3E). Most notably, a developmental time-course in tubers Most notably, a developmental time-course in tubers showed that *IbGGPPS2* expression reaches its highest level at 60 days after planting (DAP), coinciding with the key developmental stage of tuber initiation and early expansion. Subsequently, expression declines up until 120 DAP. (Fig. 3F). This temporal expression pattern closely mirrors the kinetics of carotenoid accumulation during tuber development in orange-red fleshed varieties, in which the highest carotenoid content was detected at 60 DAP [39].

In summary, our combined evidence indicates that IbGGPPS2 is a key regulator of carotenoid biosynthesis in sweet potato, a hypothesis that awaits future *in vivo* validation.

IbGGPPS2 regulates coordinated enhancement of plant growth and carotenoid biosynthesis

To elucidate the functional role of *IbGGPPS2* in carotenoid metabolism and plant development, we initially produced transgenic *Arabidopsis* lines expressing *IbGGPPS2* under the control of the strong

constitutive 35S promoter (Supplemental Fig. S5A; Fig. 4B). Analysis of three independent overexpression lines revealed a significantly accelerated flowering time, with bolting occurring approximately 5 days earlier than in WT (Fig. 4A, C). These lines also exhibited a marked reduction in rosette leaf number (Fig. 4D), a phenotypic hallmark typically associated with early flowering [40]. These observations collectively indicate that *IbGGPPS2* plays a role in promoting the transition from vegetative to reproductive growth. In parallel, carotenoid profiling revealed a marked increase in leaf carotenoid content in the overexpressing lines, ranging from 29.49% to 38.09% relative to controls (Fig. 4E), establishing a clear link between *IbGGPPS2* expression and enhanced carotenoid accumulation in a heterologous system.

To further assess the biological functions of *IbGGPPS2* in its native context, we generated transgenic overexpression lines in the high-carotenoid cultivar LS 9 (Supplemental Fig. S5B-C; Fig. 4F). Analysis of three independent transgenic events showed approximately 10-fold increase in *IbGGPPS2* transcript levels in storage roots compared to WT (Fig. 4H). Phenotypic characterization at the seedling stage revealed that *IbGGPPS2*-overexpressing plants exhibited enhanced vigor, with significant increases in plant height, stem diameter, and leaf area (Supplemental Fig. S6). At maturity, the storage roots of transgenic lines developed a more intense orange pigmentation than WT tubers (Fig. 4G), a visual indicator of altered carotenoid composition. Consistent with this observation, metabolic analyses confirmed a substantial elevation in carotenoid content in roots of overexpressing plants, with a 15.41% – 23.51% increase over control (Fig. 4I). Additionally, leaves of *IbGGPPS2* overexpressing plants exhibited a significant increase in chlorophyll content (Fig. 4J), accompanied by an elevated maximum photochemical efficiency of Photosystem II (F_v/F_m) (Fig. 4K). Further evaluation of yield-related traits revealed that the weight per plant was significantly increased in *IbGGPPS2*-overexpressing lines compared to WT (Fig. 4M), despite no significant difference in the number of storage roots per plant (Fig. 4L). These concurrent enhancements suggest *IbGGPPS2* is associated with increased storage root weight.

Collectively, these results establish *IbGGPPS2* as a key integrator of metabolism and development, coordinating enhanced carotenoid accumulation, photosynthetic efficiency, and vegetative growth to simultaneously improve both quality and yield in sweet potato.

Discussion

In this study, we produced two new sweet potato varieties, XZ 8 – 1 and LS 9 – 1, with enhanced carotenoid content and improved agronomic traits. Given the hexaploid nature of sweet potato (2n = 6x = 90) and the well-documented complexity of its genome, fully resolving the genetic architecture underlying trait variation in open-pollinated populations remains a substantial challenge [9, 10]. Nevertheless, the 40-fold carotenoid increase in XZ 8 – 1, coupled with its flesh color shift from purple to deep orange-red, suggests successful recombination or upregulation of key biosynthetic genes such as *GGPPS* and *LCYB*. The absence of xanthophylls but presence of zeaxanthin in the purple-fleshed parent—a pattern also observed among the purple-fleshed accessions within our hybrid population—implies that

XZ 8 − 1 overcame a metabolic bottleneck in the xanthophyll cycle. This extends understanding of the genetic basis of flesh color and demonstrates how open pollination can assemble favorable alleles to boost nutritional quality, relevant for addressing vitamin A deficiency [41, 42]. Meanwhile, LS 9 − 1 maintained high carotenoid levels while significantly improving yield components, breaking the typical yield-quality trade-off. Increased leaf area and branch number suggest enhanced source capacity and canopy architecture drove its productivity gains. This supports the hypothesis that yield and quality traits can be independently combined, challenging the notion of a rigid trade-off in root crops [43, 44].

The superior agronomic traits exhibited by these lines prompted a molecular investigation into the underlying mechanisms. We identified *IbGGPPS2*, a gene encoding geranylgeranyl diphosphate synthase, as a candidate contributor to the enhanced carotenoid phenotype of XZ 8 − 1. The transcript level of *IbGGPPS2* in XZ 8 − 1 was 15-fold higher than in YS 25, and strikingly, 195-fold higher than in its direct maternal parent XZ 8 (Fig. 3A), correlating with the significant increase in carotenoid content observed in XZ 8 − 1. Similarly, LS 9 − 1 exhibited a 7.5-fold increase in *IbGGPPS2* expression compared to its maternal parent LS 9 (Fig. 3A), implying that *IbGGPPS2* may play a positive role in the yield formation of LS 9 − 1. Furthermore, bacterial color complementation assays demonstrated that IbGGPPS2 possesses robust enzymatic activity catalyzing the synthesis of GGPP, an essential C20 precursor for carotenoid biosynthesis; heterologous expression of *IbGGPPS2* in *Arabidopsis* not only increased leaf carotenoid content by 29–38% but also consistently accelerated flowering time, indicating its influence on broader isoprenoid metabolism or resource allocation that impacts developmental transitions [45, 46]. Taken together, given the hexaploid nature of sweet potato, although we cannot genetically determine that *IbGGPPS2* is the direct causal factor for the improved traits in the two new varieties, it can be inferred that *IbGGPPS2* is one of the major contributors.

Most notably, overexpression of *IbGGPPS2* in sweet potato enhanced both storage root carotenoid content (15–24%) and vegetative growth (plant height, stem diameter, leaf area, and chlorophyll content), positioning *IbGGPPS2* at a critical metabolic nexus that supplies GGPP for carotenoid and photosynthesis-related pathways [47, 48]. The distinct outcomes between XZ 8 − 1 and *IbGGPPS2*-overexpressing lines reflect their different genetic backgrounds: XZ 8 − 1, derived from low-carotenoid purple-fleshed XZ 8, achieved a 40-fold increase likely through synergistic allele recombination during open pollination; while the 15–24% increase in high-carotenoid LS 9 directly confirms *IbGGPPS2*'s positive regulatory role even in a challenging high-background context. The concurrent vegetative growth enhancement suggests that increased GGPP flux extends to broader isoprenoid networks. As GGPP is a shared precursor for gibberellins and strigolactones—key regulators of stem elongation, leaf expansion, and branching—growth promotion may involve GGPP rerouting toward these hormone pathways [28], with elevated chlorophyll content and photosynthetic efficiency (Fig. 4J-K) providing additional energy and carbon skeletons. Thus, *IbGGPPS2* coordinates systemic growth enhancement through dual effects: hormone precursor supply and improved photosynthetic capacity, demonstrating that fortifying this upstream isoprenoid node can break the typical yield-quality trade-off.

In conclusion, this study provides an integrated breeding and molecular framework to develop high-carotenoid, high-yielding sweet potato varieties by combining conventional hybridization with functional gene analysis. It identified valuable germplasm and a key regulatory gene while providing insights into the coordinated regulation of carotenoid metabolism and plant growth in sweet potato. These findings pave the way for the rational design of crop varieties with optimized nutritional and agronomic traits.

Declarations

Ethics Approval and Consent to Participate Not applicable. This study does not involve human participants, human data, or human tissue, nor does it involve any animal experiments. The plant materials used are leading commercial cultivars, widely cultivated and readily available from commercial sources. Their use complies with relevant institutional, national, and international guidelines, including the research exemption clauses of applicable seed laws. This study does not involve any endangered or protected species listed under the Convention on International Trade in Endangered Species of Wild Fauna and Flora (CITES). Therefore, no ethical approval or consent to participate was required.

Consent to Publish Declaration All authors have reviewed and approved the final version of the manuscript and unanimously agree to its submission to this journal for publication.

Data Availability Statement All data and materials generated or analyzed during this study are available within the manuscript and its supplementary files. Additional requests for information may be directed to the corresponding author. The IbGGPPS2 gene sequence data generated and/or analysed during the current study are available in the Genome Sequence Archive (GSA) repository.

Authorship Contribution JG, YD and HL conceived the study. YZ and YG provided sweet potato hybridization populations. PZ performed the transformation of sweet potato overexpressing lines. PZ, JL, YG, YF and MY performed the other experiments. JG, YD and HL analyzed the data. HL wrote the manuscript. JG, YD, RJ, LK, CZ, JK and WW revised the manuscript. All authors approved the submitted version.

Funding The research was Sponsored by Natural Science Foundation of Henan (252300423026), the National Natural Science Foundation of China (U2004143) and the Education Department of Hainan Province (Hnjg2024ZD-86).

Declaration of Competing Interests The authors affirm that there are no known financial or personal relationships that could be construed as influencing the work presented in this manuscript.

References

1. Behera S, Chauhan VBS, Pati K, Bansode V, Nedunchezhiyan M, Verma AK, Monalisa K, Naik PK, Naik SK. Biology and biotechnological aspect of sweet potato (*Ipomoea batatas* L.): a commercially important tuber crop. Planta. 2022;256(2):40.

2. Kang L, Park S, Ji CY, Kim HS, Lee H, Kwak S. Metabolic engineering of carotenoids in transgenic sweetpotato. Breed Sci. 2017;67(1):27–34.
3. Liu Y, Chen Q, Zhou M, Yang X, Yang C, Jiao C. Sweet potato study in China: stress response mechanisms, molecular breeding, and productivity. J Plant Physiol. 2020;254:153283.
4. Xiao Y, Zhu M, Gao S. Genetic and genomic research on sweet potato for sustainable food and nutritional security. Genes 2022, 13(10).
5. Escobar-Puentes AA, Palomo I, Rodriguez L, Fuentes E, Villegas-Ochoa MA, Gonzalez-Aguilar GA, Olivas-Aguirre FJ, Wall-Medrano A. Sweet potato (*Ipomoea batatas* L.) phenotypes: from agroindustry to health effects. *Foods* 2022, 11(7).
6. Wang S, Nie S, Zhu F. Chemical constituents and health effects of sweet potato. Food Res Int. 2016;89:90–116.
7. Gurmu F, Hussein S, Laing M. Self- and cross-incompatibilities in sweetpotato and their implications on breeding. Aust J Crop Sci. 2013;7(13):2074–8.
8. Yan M, Li M, Wang Y, Wang X, Moeinzadeh M, Quispe-Huamanquispe DG, Fan W, Fang Y, Wang Y, Nie H, et al. Haplotype-based phylogenetic analysis and population genomics uncover the origin and domestication of sweetpotato. Mol Plant. 2024;17(2):277–96.
9. Yan M, Nie H, Wang Y, Wang X, Jarret R, Zhao J, Wang H, Yang J. Exploring and exploiting genetics and genomics for sweetpotato improvement: status and perspectives. Plant Commun. 2022;3(5):100332.
10. Yang J, Moeinzadeh M, Kuhl H, Helmuth J, Xiao P, Haas S, Liu G, Zheng J, Sun Z, Fan W, et al. Haplotype-resolved sweet potato genome traces back its hexaploidization history. Nat Plants. 2017;3(9):696–703.
11. Drapal M, Fraser PD. Determination of carotenoids in sweet potato (*Ipomoea batatas* L., Lam) tubers: implications for accurate provitamin A determination in staple sturdy tuber crops. Phytochemistry. 2019;167:112102.
12. Beltrán J, Wurtzel ET. Carotenoids: resources, knowledge, and emerging tools to advance apocarotenoid research. Plant Sci. 2025;350:112298.
13. Hou X, Rivers J, León P, McQuinn RP, Pogson BJ. Synthesis and function of apocarotenoid signals in plants. Trends Plant Sci. 2016;21(9):792–803.
14. Nisar N, Li L, Lu S, Khin NC, Pogson BJ. Carotenoid metabolism in plants. Mol Plant. 2015;8(1):68–82.
15. Sierra J, McQuinn RP, Leon P. The role of carotenoids as a source of retrograde signals: impact on plant development and stress responses. J Exp Bot. 2022;73(21):7139–54.
16. Wurtzel ET. Changing form and function through carotenoids and synthetic biology. Plant Physiol. 2019;179(3):830–43.
17. Maoka T. Carotenoids as natural functional pigments. J Nat Med. 2020;74(1):1–16.

18. Bas TG. Bioactivity and bioavailability of carotenoids applied in human health: technological advances and innovation. Int J Mol Sci. 2024;25(14):7603.
19. Eggersdorfer M, Wyss A. Carotenoids in human nutrition and health. Arch Biochem Biophys. 2018;652:18–26.
20. Milani A, Basirnejad M, Shahbazi S, Bolhassani A. Carotenoids: biochemistry, pharmacology and treatment. Br J Pharmacol. 2017;174(11):1290–324.
21. Islam SN, Nusrat T, Begum P, Ahsan M. Carotenoids and β-carotene in orange fleshed sweet potato: a possible solution to vitamin A deficiency. Food Chem. 2016;199:628–31.
22. Kurabachew H. The role of orange fleshed sweet potato (*Ipomoea batatas*) for combating vitamin A deficiency in Ethiopia: a review. Int J Food Sci Nutr Eng. 2015;3(5):141–6.
23. Neela S, Fanta SW. Review on nutritional composition of orange-fleshed sweet potato and its role in management of vitamin A deficiency. Food Sci Nutr. 2019;7(6):1920–45.
24. Moreno JC, Mi J, Alagoz Y, Al Babili S. Plant apocarotenoids: from retrograde signaling to interspecific communication. Plant J. 2021;105(2):351–75.
25. Sun T, Rao S, Zhou X, Li L. Plant carotenoids: recent advances and future perspectives. Mol Hortic. 2022;2(1):3–21.
26. Beck G, Coman D, Herren E, Ruiz-Sola MÁ, Rodríguez-Concepción M, Gruissem W, Vranová E. Characterization of the GGPP synthase gene family in *Arabidopsis thaliana*. Plant Mol Biol. 2013;82(4–5):393–416.
27. Song S, Jin R, Chen Y, He S, Li K, Tang Q, Wang Q, Wang L, Kong M, Dudareva N, et al. The functional evolution of architecturally different plant geranyl diphosphate synthases from geranylgeranyl diphosphate synthase. Plant Cell. 2023;35(6):2293–315.
28. Barja MV, Rodriguez-Concepcion M. Plant geranylgeranyl diphosphate synthases: every (gene) family has a story. *aBIOTECH* 2021, 2(3):289–298.
29. Zhou F, Wang C, Gutensohn M, Jiang L, Zhang P, Zhang D, Dudareva N, Lu S. A recruiting protein of geranylgeranyl diphosphate synthase controls metabolic flux toward chlorophyll biosynthesis in rice. Proc Natl Acad Sci USA. 2017;114(26):6866–71.
30. Barja MV, Ezquerro M, Beretta S, Diretto G, Florez-Sarasa I, Feixes E, Fiore A, Karlova R, Fernie AR, Beekwilder J, et al. Several geranylgeranyl diphosphate synthase isoforms supply metabolic substrates for carotenoid biosynthesis in tomato. New Phytol. 2021;231(1):255–72.
31. Wang Q, Huang X, Cao T, Zhuang Z, Wang R, Lu S. Heteromeric geranylgeranyl diphosphate synthase contributes to carotenoid biosynthesis in ripening fruits of red pepper (*Capsicum annuum* var. conoides). J Agric Food Chem. 2018;66(44):11691–700.
32. Ezquerro M, Li C, Perez-Perez J, Burbano-Erazo E, Barja MV, Wang Y, Dong L, Lison P, Lopez-Gresa MP, Bouwmeester HJ, et al. Tomato geranylgeranyl diphosphate synthase isoform 1 is involved in the stress-triggered production of diterpenes in leaves and strigolactones in roots. New Phytol. 2023;239(6):2292–306.

33. Rao S, Cao H, O Hanna FJ, Zhou X, Lui A, Wrightstone E, Fish T, Yang Y, Thannhauser T, Cheng L, et al. Nudix hydrolase 23 post-translationally regulates carotenoid biosynthesis in plants. Plant Cell. 2024;36(5):1868–91.
34. Zhang W, Zuo Z, Zhu Y, Feng Y, Wang Y, Zhao H, Zhao N, Zhang H, He S, Liu Q, et al. Fast track to obtain heritable transgenic sweet potato inspired by its evolutionary history as a naturally transgenic plant. Plant Biotechnol J. 2023;21(4):671–3.
35. Guo Y, Zou L, Huang L, Li H, Yang RH, Li K, Zhang C, Liu Y, Shen M, Zhao D et al. Overexpression of *GhGGPPS10* and *GhGGPPS23* enhances plant biomass accumulation and optimizes photosynthetic performance in cotton. Plant Cell Environ 2025:10–1111.
36. Miyake C, Amako K, Shiraishi N, Sugimoto T. Acclimation of tobacco leaves to high light intensity drives the plastoquinone oxidation system-relationship among the fraction of open PSII centers, non-photochemical quenching of Chl fluorescence and the maximum quantum yield of PSII in the dark. Plant Cell Physiol. 2009;50(4):730–43.
37. Lihong Liu ZSMZ, Wang YLAQ. Improvement of carotenoid accumulation in tomato fruit. Phytonutritional Improv Crops 2017.
38. Dong C, Qu G, Guo J, Wei F, Gao S, Sun Z, Jin L, Sun X, Rochaix JD, Miao Y, et al. Rational design of geranylgeranyl diphosphate synthase enhances carotenoid production and improves photosynthetic efficiency in *Nicotiana tabacum*. Sci Bull. 2022;67(3):315–27.
39. Zhang J, He L, Dong J, Zhao C, Wang Y, Tang R, Wang W, Ji Z, Cao Q, Xie HE, et al. Integrated metabolic and transcriptional analysis reveals the role of carotenoid cleavage dioxygenase 4 (IbCCD4) in carotenoid accumulation in sweetpotato tuberous roots. Biotechnol Biofuels Bioprod. 2023;16(1):45.
40. Chen W, Wang T, Li X, Feng J, Liu Q, Xu Z, You Q, Yang L, Liu L, Chen S, et al. *Arabidopsis* RGLG1/2 regulate flowering time under different soil moisture conditions by affecting the protein stability of TOE1/2. New Phytol. 2025;246(4):1609–26.
41. Amagloh FK, Coad J. Orange-fleshed sweet potato-based infant food is a better source of dietary vitamin A than a maize-legume blend as complementary food. Food Nutr Bull. 2014;35(1):51–9.
42. Gurmu F, Hussein S, Laing M. The potential of orange-fleshed sweet potato to prevent vitamin A deficiency in Africa. Int J Vitam Nutr Res. 2014;84(1–2):65–78.
43. Kwak S. Biotechnology of the sweetpotato: ensuring global food and nutrition security in the face of climate change. Plant Cell Rep. 2019;38(11):1361–3.
44. Sapakhova Z, Raissoova N, Daurov D, Zhapar K, Daurova A, Zhigailov A, Zhambakin K, Shamekova M. Sweet potato as a key crop for food security under the conditions of global climate change: a review. Plants. 2023;12(13):2516.
45. Gawarecka K, Ahn JH. Isoprenoid-derived metabolites and sugars in the regulation of flowering time: does day length matter? Front Plant Sci. 2021;12:765995.
46. Lange I, Lange BM, Navarre DA. Altering potato isoprenoid metabolism increases biomass and induces early flowering. J Exp Bot. 2020;71(14):4109–24.

47. Dong C, Zhang M, Song S, Wei F, Qin L, Fan P, Shi Y, Wang X, Wang R. A small subunit of geranylgeranyl diphosphate synthase functions as an active regulator of carotenoid synthesis in *Nicotiana tabacum*. Int J Mol Sci. 2023;24(2):992.
48. Ruiz-Sola MÁ, Barja MV, Manzano D, Llorente B, Schipper B, Beekwilder J, Rodriguez-Concepcion M. A single *Arabidopsis* gene encodes two differentially targeted geranylgeranyl diphosphate synthase isoforms. Plant Physiol. 2016;172(3):1393–402.

Figures

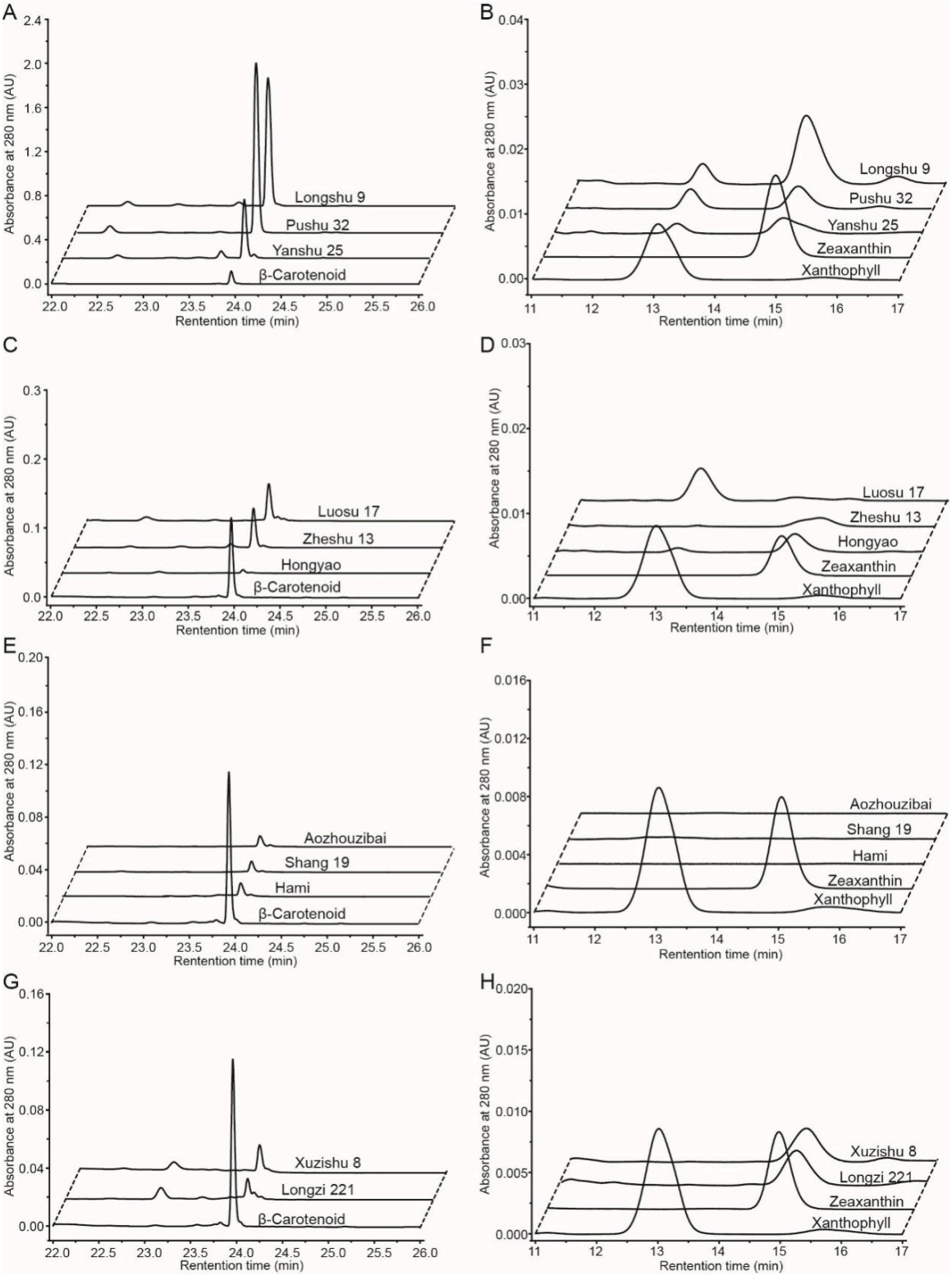

Figure 1

Carotenoid composition and relative content in sweet potato tubers with different flesh colors determined by liquid chromatography. **A-B** Relative content of β-carotene, xanthophyll and zeaxanthin in orange-red fleshed tubers. **C-D**Relative content of β-carotene, xanthophyll and zeaxanthin in yellow fleshed tubers. **E-F** Relative content of β-carotene, xanthophyll and zeaxanthin in white fleshed tubers. **G-H** Relative content of β-carotene, xanthophyll and zeaxanthin in purple fleshed tubers.

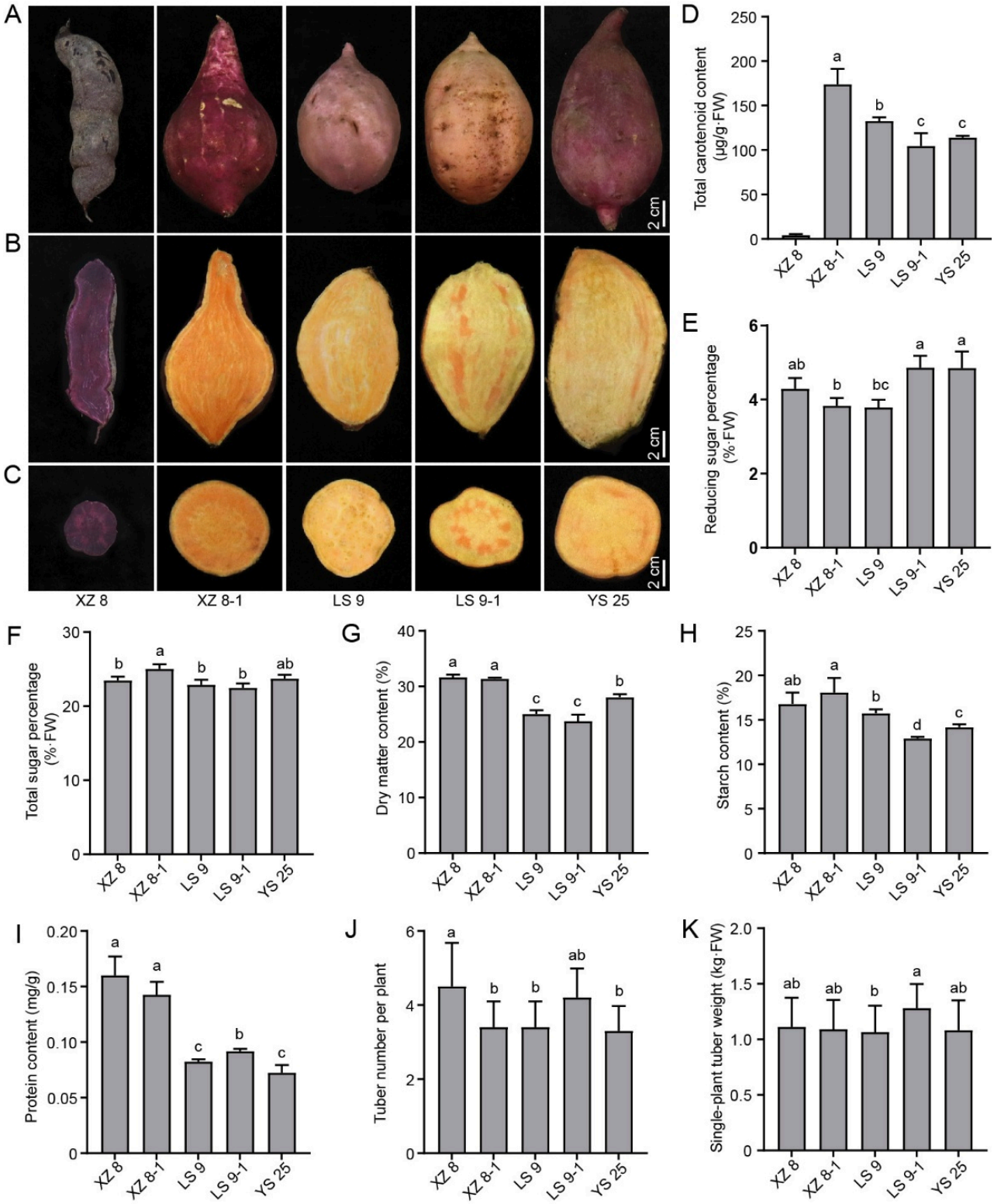

Figure 2

Agronomic and phytochemical traits of tubers in the novel sweet potato varieties XZ 8-1 and LS 9-1 versus their maternal parents and the control YS 25. **A-C** Representative images of tubers: overall morphology, longitudinal section morphology, cross section morphology. **D** Total carotenoid content of the different genotypes. n = 3. **E** Dry matter content. n = 3. **F** Starch content. n = 3. **G**Protein content. n = 3. **H** Reducing sugar content. n = 3. **I** Total sugar content. n = 3. **J** Tuber number per plant. n = 10. **K** Fresh

total tuber weight per plant. n = 10. Data is presented as mean ± SD. Different lowercase letters indicate statistically significant differences among genotypes ($p < 0.05$) as determined by one-way ANOVA with Tukey's post-hoc test. Scale bar, 2 cm.

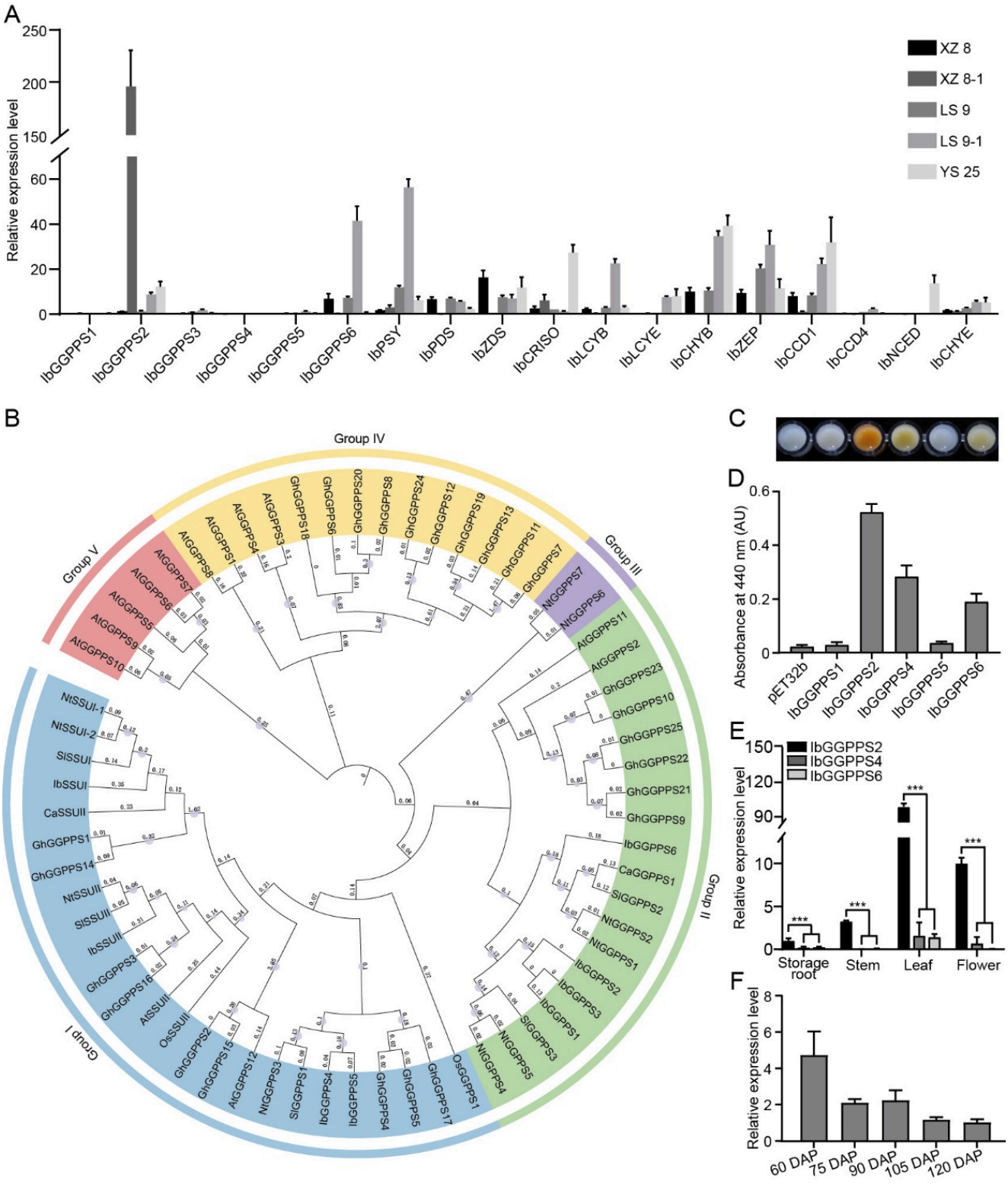

Figure 3

Identification of *IbGGPPS2* as a candidate gene involved in carotenoid biosynthesis in sweet potato storage roots. **A** Relative expression levels of carotenoid metabolic genes in the storage roots of the high-carotenoid cultivar XZ 8, XZ 8-1, LS 9, LS 9-1 and YS 25 determined by qRT-PCR. **B** Phylogenetic analysis of GGPPS proteins from sweet potato and other plant species. The six identified IbGGPPS proteins cluster into two subfamilies (III and IV). **C** Characterization of IbGGPPS enzyme activity using a bacterial pigment complementation assay. Representative images of *E. coli* colonies expressing different *IbGGPPS*genes are shown. **D** Spectrophotometric quantification of yellow color in the *E. coli* strains shown in **C**. **E** Tissue-specific expression patterns of *IbGGPPS2*, *IbGGPPS4*, and *IbGGPPS6* in sweet potato. Transcript levels were analyzed in tubers, stems, leaves, and flowers by qRT-PCR. **F** Expression profile of *IbGGPPS2*during tuber development at 60, 75, 90, 105, and 120 DAP. Data represent mean absorbance values ± SD, n = 3, ***$p < 0.001$.

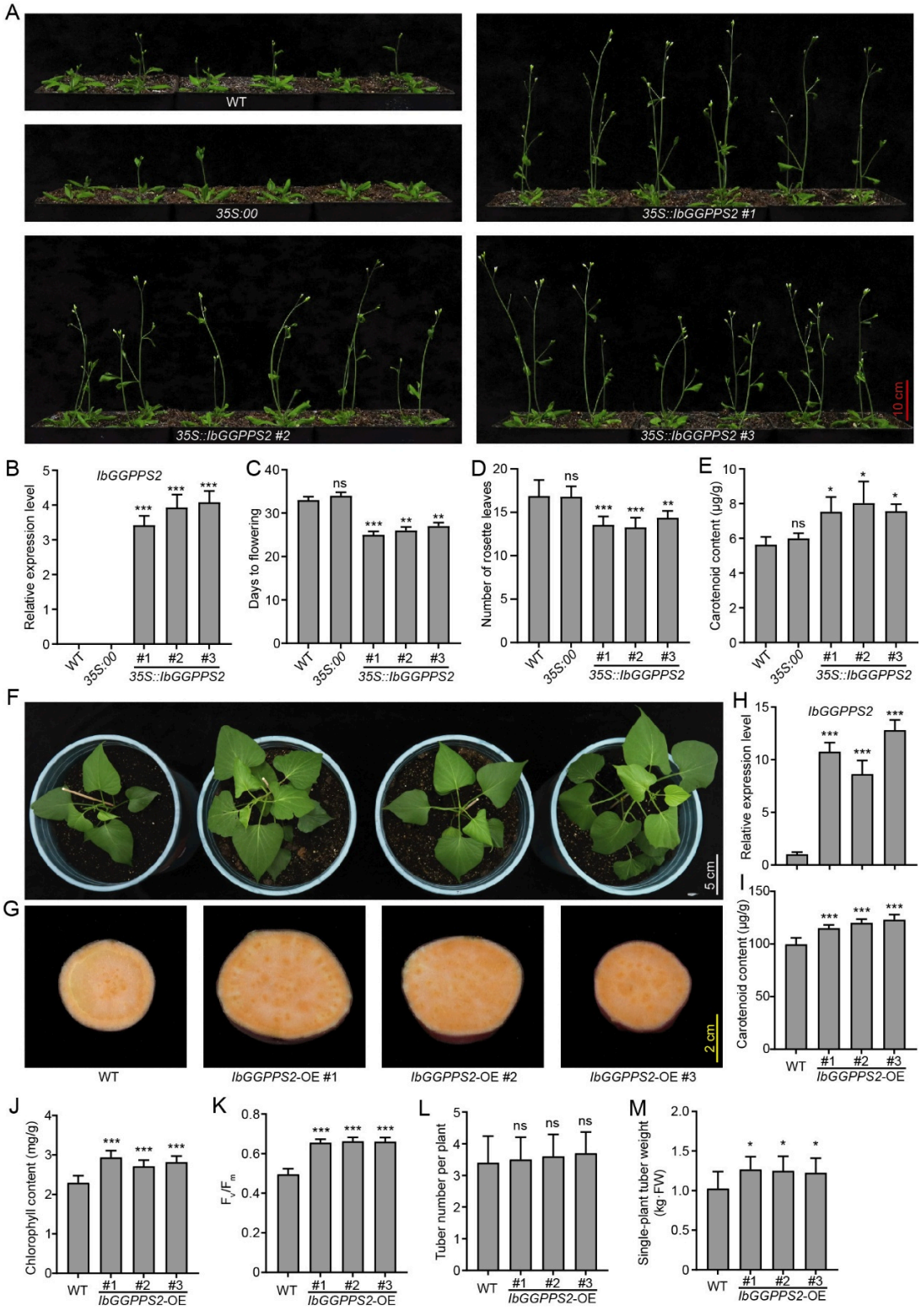

Figure 4

Overexpression of IbGGPPS2 enhances plant growth and carotenoid biosynthesis in *Arabidopsis* and sweet potato. **A** Phenotypes of WT and *IbGGPPS2*-overexpressing (*35S::IbGGPPS2*) *Arabidopsis* plants of the same age. Scale bar, 10 cm. **B** Relative *IbGGPPS2* gene expression levels measured by qRT-PCR in transgenic *Arabidopsis* lines. **C** Bolting time in WT and *35S::IbGGPPS2 Arabidopsis* plants. n = 10. **D** Number of rosette leaves in WT and *35S::IbGGPPS2 Arabidopsis* plants. n = 10. (E) Total carotenoid

content in leaves of WT and *35S::IbGGPPS2 Arabidopsis* plants. n = 10. **F** Plant architecture of 20-day-old WT sweet potato seedlings and three independent *IbGGPPS2* overexpressing (*IbGGPPS2*-OE) lines. Scale bar, 5 cm. **G** Storage root cross-sections of WT and three independent *IbGGPPS2*-OE sweet potato lines at maturity. Scale bar, 2 cm. **H** Relative *IbGGPPS2* expression levels in storage roots of WT and transgenic sweet potato lines (n = 3). **I-K** Total carotenoid content in storage roots, chlorophyll content and primary light energy conversion efficiency of PSII (F_v/F_m) in leaves of WT and *IbGGPPS2*-OE transgenic sweet potato plants. **I** Total carotenoid content, **J** Chlorophyll content, **K** Primary light energy conversion efficiency of PSII (F_v/F_m). **L** Tuber number per plant. **M** Fresh total tuber weight per plant. n = 10. Data is presented as mean ± SD, **p* < 0.05, ***p* < 0.01, ****p* < 0.001.

Supplementary Files

This is a list of supplementary files associated with this preprint. Click to download.

- IbGGPPS2sequenceinformation.docx
- SupplementalFigs.docx